Pharmacological intervention to restore connectivity deficits of neuronal networks derived from ASD patient iPSC with a TSC2 mutation

Mouhamed Alsaqati
Cardiff University
Vivi M Heine
Vrije Universiteit Amsterdam
Adrian J. Harwood (HarwoodAJ@cardiff.ac.uk)
Cardiff University https://orcid.org/0000-0003-3124-5169

Research

Keywords: Tuberous sclerosis complex (TSC), mechanistic target of rapamycin complex 1 (mTORC1), Multi-electrode array (MEA), induced Pluripotent Stem Cell (iPSC)

Posted Date: June 17th, 2020

DOI: https://doi.org/10.21203/rs.3.rs-35221/v1

Version of Record: A version of this preprint was published on October 19th, 2020. See the published version at https://doi.org/10.1186/s13229-020-00391-w.

Abstract

Background

Tuberous sclerosis complex (TSC) is a rare genetic multisystemic disorder resulting from autosomal dominant mutations in the *TSC1* or *TSC2* genes. It is characterised by hyperactivation of the mechanistic target of rapamycin complex 1 (mTORC1) pathway and has severe neurodevelopmental and neurological components including autism, intellectual disability and epilepsy. In human and rodent models, loss of the TSC proteins causes neuronal hyperexcitability and synaptic dysfunction, although the consequences of these changes for the developing central nervous system is currently unclear.

Methods

Here we apply Multi-electrode array (MEA)-based assays to study the effects of TSC2 loss on neuronal network activity using Autism Spectrum Disorder (ASD) patient-derived iPSCs. We examine both temporal synchronisation of neuronal bursting, and spatial connectivity between electrodes across the network.

Results

We find that TSC2 patient-derived neurons with a functional loss of *TSC2*, in addition to possessing neuronal hyperactivity, develop a dysfunctional neuronal network with reduced synchronisation of neuronal bursting and lower spatial connectivity. These deficits of network function are associated with elevated expression of genes for inhibitory GABA signalling and decreased expression of those for glutamate signalling, indicating an imbalance of synaptic inhibitory-excitatory signalling. mTORC1 activity functions within a homeostatic triad of protein kinases, AMP-dependent protein Kinase 1 (AMPK), mTORC1 and Unc-51 like Autophagy Activating Kinase 1 (ULK1) that orchestrate the interplay of anabolic cell growth and catabolic autophagy while balancing energy and nutrient homeostasis. The mTORC1 inhibitor rapamycin suppresses neuronal hyperactivity, but does not increase network activity, whereas activation of AMPK restores network activity without affecting the network burst length or regularity. In contrast, the ULK1 activator, LYN-1604 increases the network behaviour, shortens the network burst lengths, and reduces the number of uncorrelated spikes.

Limitations

Although a robust and consistent phenotype is observed across multiple independent iPSC clones, the results are based on iPSC from one patient. There may be more subtle differences between patients with different *TSC2* mutations or differences of polygenic background within their genomes. This may affect the severity of the network deficit or the pharmacological response between TSC2 patients.

Conclusions

Our observations suggest that there is a reduction in the network connectivity of the *in vitro* neuronal network associated with ASD patients with *TSC2* mutation, which may arise via an excitatory/inhibitory

imbalance due to increased GABA signalling at inhibitory synapses. This deficit can be effectively suppressed via activation of ULK1.

Background

Tuberous sclerosis complex (TSC) is a developmental genetic disorder characterised by the widespread progression of benign tumors in multiple organs. It affects approximately 1:6000 individuals and is caused by mutations in either *TSC1* or *TSC2* [1]. The most common neurological symptoms associated with TSC are: epilepsy which occurs in 80-90% of patients and is often unmanageable; autism spectrum disorder (ASD) which occurs in 61% of patients, and intellectual disability [1]. The TSC1 and TSC2 proteins form a heterodimer complex that binds to a third subunit (TBC1D7) to form the TSC complex. This complex acts as a GTPase activating protein (GAP). TSC2 protein consists of the GAP domain and most phosphorylation sites, whereas the TSC1 acts as a stabiliser of the complex and prevents TSC2 degradation [2]. Both TSC1 and TSC2 are involved in the stability of the complex and for that reason patients with either gene mutation present with similar clinical phenotypes. The main role of the TSC complex is the regulation of mechanistic target of rapamycin (mTOR) that exists as two functionally distinct complexes termed, mTOR complex 1 and 2 (mTORC1 and mTORC2) [3]. The mTORC1 pathway plays key roles in multiple cellular processes; such as cell growth and division; autophagy, and transcription [4, 5]. Loss of *TSC1* or *TSC2* function activates mTOR signalling, which results in an mTORC1-dependent increase of ribosomal protein S6 (rpS6), rpS6 kinase 1 (S6K1) eukaryotic initiating factor 4E-binding protein 1 (4E-BP1) phosphorylation [6, 7]. Aberrant mTORC1 signalling has been identified in cancer progression, diabetes and aging, and is involved in increasing cell growth and proliferation [2, 8].

Reports demonstrate that mTORC1 signalling hyperactivation in neurons is associated with aberrant axonal and dendritic connectivity, enlarged soma size, increased cellular stress, reduced myelination, synaptic dysfunction and neuronal hyperexcitability [9-12]. In animal models, treatment with mTORC1 inhibitor, rapamycin recovered the behavioural deficits including learning, memory, and autistic-like features and the neuronal hyperexcitability [13-15]. In human models, rapamycin reversed neuronal hyperexcitability and improved recall memory in patients with angiomyolipomas associated with TSC [16-18]. However, other neuropsychological measures including executive functions and recognition memory showed reduction in some participants [18]. Additionally, rapamycin did not ameliorate neurocognitive dysfunction or behavioural issues in children with TSC [18].

Accumulating reports have suggested that there is a link between Unc-51 Like Autophagy Activating Kinase 1 (ULK1) and mTORC1 in mammalian cells. Studies showed that mTORC1 inhibits ULK1 activation by phosphorylating Ser-757 of ULK1 and disrupting its interaction with AMP-dependent protein Kinase 1 (AMPK) and destabilises ULK1 [19, 20]; the latter is known to activate the TSC1/TSC2 complex formation and suppress mTORC1 signalling [21, 22]. While, activation of ULK1 through phosphorylation of Ser-317 and Ser-777 results in ULK1-AMPK interaction and phosphorylation of Raptor on multiple sites by both AMPK and ULK1 [19, 20] that potently inhibits substrate binding to mTORC1 to block

downstream signalling. The interplay between mTORC1-AMPK-ULK1 highlights a potential signalling mechanism to reverse the defects of hyperactive mTORC1 in TSC-disease cells, i.e., through manipulating the ULK1-AMPK interaction to reduce mTORC1 activity.

In this study, we examined the neuronal network behaviour in TSC2 patient-derived neurons with loss of *TSC2* function, and we used a novel approach to rescue their abnormal activity. The neuronal hyperexcitability was reversed by rapamycin, while the synaptic dysfunction was not sensitive to rapamycin treatment. Treatment with the ULK1 activator ameliorated the synaptic activity of *TSC2* patient neurons and improved their synchronicity. This strategy of restoring disease state could be further developed as a new treatment for TSC patients.

Methods

Cell cultures

TSC patient and control fibroblasts (C3, GM23973) were obtained from the Coriell Biorepository (all teenage donors), and controls C1 (infant) and C2 (teenage) were obtained from anonymous control donors. The selected TSC patient was reported with mental retardation and seizures along with other TSC-related abnormalities. iPSC reprogramming was done based on polycistronic construct with *OCT3/4*, *c-MYC*, *SOX2*, and *KLF4* [23]. All the iPSC lines were cultured in Essential 8 medium (Gibco) on Geltrex LDEV-free (Gibco). Generation of in-direct contact iPSC-neuronal cultures was performed as described earlier [24] with slight modifications. Neuronal cultures with a density of 62.5 K/2.0 cm^2 were maintained in the medium contained neurobasal composition with brain-derived neurotrophic factor (BDNF) (20 ng/mL; Peprotech) and cAMP (1 μM; Sigma). At day 45 of differentiation some cultures were treated with 10nM rapamycin for the remainder of the cultures. To promote maturation neurons were treated with CultureOne™ Supplement (Cat No. A3320201) at day50 of differentiation for two days. At day 60 of differentiation, $TSC^{-/+}$ and control neurons were plated on the MEAs.

Multiple Electrode Arrays (MEAs)

All experiments were performed using CytoView MEA 24-well plates (M384-tMEA-24W, 4X4 electrode grid). MEAs were first pre-treated with 0.01% polyethylenimine (Sigma) and incubated for 1 hour at 37°C. Day 60 neurons were plated as high density drop cultures (5,000 cells/μL) containing 10μg/ml laminin. After 1 hour, conditioned medium was added into each MEA and after 24 hours 0.5ml of fresh BrainPhys media was added to each array. MEA cultures were maintained in 1:1 fresh to astrocyte condition BrainPhys media replaced every 3-4 days. Electrophysiological activity was recorded every 10 days using hardware (Maestro Pro complete with Maestro 768channel amplifier) and software (AxIS 1.5.2) from Axion Biosystems (Axion Biosystems Inc., Atlanta, GA). Channels were sampled simultaneously with a gain of 1000× and a sampling rate of 12.5 kHz/channel. During the recording, the temperature was maintained constant at 37°C.

For drug treatment, LYN-1604 were purchased from Cambridge Bioscience (Cambridge, UK), rapamycin were purchased from Sigma-Aldrich (St. Louis, MO, USA), CNQX, APV, kainic acid and bicuculline from R&D System (R&D System Inc., Minneapolis, MN, USA), GABA, diazepam, ACIAR, diltiazem and DMCM were purchased from Tocris (Bio-Techne Ltd.). Stock concentrations were diluted as required in 1 mL 1:1 BrainPhys:BrainPhys ACM. Medium containing diluted drugs were added to MEAs and subsequently incubated for 10 mins at 37 °C in a standard 5% CO2 incubator environment unless otherwise stated. After recordings, medium was removed from MEAs and cultures were washed 3 times with PBS. 1 ml of fresh medium was then added, and cultures were incubated for 10 minutes as before. This medium was then removed and replaced with fresh medium and recorded again.

A Butterworth band-pass filter (with a high-pass cut-off of 200 Hz and low-pass cut-off of 3000Hz) was applied along with a variable threshold spike detector set at 5.5× standard deviation on each channel. Offline analysis was achieved with custom scripts written in MATLAB (available on request). Briefly, spikes were detected from filtered data using an automatic threshold-based method set at -5.5 x σ, where σ is an estimate of the noise of each electrode based upon the median absolute deviation 1. Spike timestamps were analysed to provide statistics on the general excitability of cultures. Neuronal bursting was detected based on three parameters: inter-burst period longer than 200ms, more than 3 spikes in each burst and a maximum inter-spike (intra-burst) interval of 300 milliseconds. Network activity was illustrated by creating array–wide spike detection rate (ASDR) plots with a bin width of 200 ms. Heat map for spatially correlated neurons on the MEAs were generated with MATLAB imagesc function using in-house scripts. In the heat maps, a dark red-dark blue colour scale was used whereby shades of red and blue represented higher and lower correlations, respectively, for control or TSC2 neurons plated on the 16 electrode-grid.

RNA extraction and quantitative (q)PCR

Cells were lysed with QIAzol Lysis Reagent (Life Technologies) and stored at -20 °C. Total RNA was extracted from hiPSCs-derived TSC and control neuron lysates using the miRNeasy mini kit (reference 217004, Qiagen, Germany). For each sample, 1µg of total RNA was reverse transcribed using the miScript II RT Kit (Qiagen). For qPCR analysis QuantiTect SYBR Green PCR kit (Qiagen, Germany) was employed and samples were run on a StepOnePlus™ Real-Time PCR System (Applied Biosystems) following the manufacturer's instructions. All reactions were performed in triplicate for each sample. The relative expression levels of the miRNAs and other genes was calculated using the $2^{-\Delta\Delta CT}$ method [25] and the data were normalized to *GAPDH* and *Colrf43*. The primer sequences for all genes examined in the current study are listed in Table S1.

Statistical analysis

Prism 8.0 (GraphPad Software) was used for the statistical analysis. Data shown are the mean ± s.e.m. with $P < 0.05$ considered statistically significant. Two-tailed unpaired/paired t-tests were used for

comparisons between two groups. Data distribution was assumed to be normal, but this was not formally tested.

Results

TSC2 patient iPSCs-derived neurons exhibit higher neuronal excitability but decreased synchronicity

In previous work, we reported enhanced excitability of neurons derived iPSC generated from ASD patients with *TSC1* or *TSC2* mutations [17]. In these experiments, mature neurons exhibited increased spontaneous calcium influx frequencies and an increased firing rate of TSC patient-derived neurons plated on MEAs as compared to control neurons [17]. In the current study, we have investigated the synchronisation and connectivity of neuronal network activity of differentiated patient iPSC cells lacking functional *TSC2*, due to a single nucleotide duplication (1563dupA) leading to a frameshift mutation H522T [17]. Multiple iPSC clones were obtained from each patient and control fibroblast line and verified by sequencing and characterised by immunostaining as previously shown [17].

Control and patient iPSCs were differentiated into functional neurons and plated onto MEA plates at ~day 60 and developed further to form activity neuronal networks. Spike detection from filtered raw voltage recording were generated from each electrode via the threshold-based method of QuianQuiroga and colleagues [26] and following quality control spikes were time-stamped for subsequent analysis. As previously reported, spontaneous activity of cultures on MEAs differed between control and *TSC2* mutated patient neurons (Fig. 1a, b) with increased spontaneous firing rates and higher total numbers of single unit bursts in *TSC2* neurons, with 0.9 ± 0.2 Hz, 273.1 ± 68.81 bursts, respectively compared to the control values of 0.16 Hz ± 0.07 Hz, 57.67 ± 46.76 bursts, respectively ($p < 0.01$, $p < 0.05$, unpaired t-test, Fig. 1c).

After 20 days on MEAs, synchronised bursting emerges, where multiple electrodes across the array simultaneously detect burst firing. Control neuronal cultures develop a regular pattern of synchronised bursts (SBs) separated by intervals of similar length, consistent with that previously reported [27] (Fig. 1a, b). In *TSC2* mutated patient neurons, there was a significant reduction in SB frequency (Fig. 1a, b). For example, at 40DPP (Days Post Plating) the number of SBs was significantly lower in *TSC2* neurons, 4.5 ± 1.55 SBs as compared to control neurons, 22.67 ± 4.4 SBs ($p < 0.01$, unpaired t-test, Fig. 1d). Consistent with elevated general spontaneous activity in TSC2 neurons, the firing rate within the *TSC2* SBs was higher; for example, at 40DPP the SB firing rate in *TSC2* neurons was 282.3 ± 77.04 Hz as compared to 13.67 ± 2.33 Hz in control neurons ($p < 0.05$, unpaired t-test, Fig. 1d). This suggests that although a higher intrinsic neuronal activity is present in *TSC2* neurons, it is not reflected in increased synchronised activity within the neuronal network, and in fact there exists a previously undetected deficit in network behaviour of the patient neurons.

To probe further we investigated how the pattern of neuronal firing differed between control and *TSC2* neurons. As would be predicted, the percentage of firing spikes occurring outside SBs was significantly higher in *TSC2* neurons (78.44 ± 8.5% in *TSC2* neurons as compared to 38.5 ± 9.8% in control neurons (*p*

< 0.05, unpaired t-test, Fig. 1e), Significantly, this is accompanied by a large increase in the interval between SB for *TSC2* neurons compared to controls; at 40DPP there was an approx. 5.8-fold increase of SB interval in *TSC2* cultures (151.5 ± 50.21 v 26.67 ± 4.37 s, *p < 0.01*, unpaired t-test), (Fig. 1f). When SBs do occur in the *TSC2* neurons, they persisted for longer period compared to those in control neurons; approx. 2.9-fold longer at 40 DPP than those in the control (1.25 ± 0.13 s, 3.65 ± 0.54 s (*p < 0.01*, unpaired t-test), (Fig. 1f). Finally, we investigated the variation inherent to the dataset representing the SB intervals in *TSC2* neurons as compared to the control. Whilst, the SBs in control cells exhibited a regular defined pattern with intervals that are tightly clustered around the mean, the distribution of the intervals in *TSC2* neurons are more dispersed (Fig. 1g). Combined these data indicate that although the SBs of *TSC2* neurons have more persistent and have higher firing rates, their spontaneous frequency is significantly reduced and disorganised. This pattern is well illustrated in Fig. 1b.

The reduced synchronicity seen in the *TSC2* neuronal networks is suggestive of a lower connectivity between groups of neurons. To pursue this observation, we interrogated how the neuronal spatial connectivity may differ between the control and *TSC2* neurons plated on MEAs by plotting correlation matrices between all electrodes in the MEA. In control neurons, we observed a high firing correlation between the majority of the electrodes in the cultures, represented as red and dark red pixels in Fig 1h, indicative of high level of neuronal connectivity. The firing correlation is substantially reduced for *TSC2* plated neurons, showing a loss of neuronal spatial connectivity.

Pharmacological profiling of *TSC2* patient-derived neuronal networks

To establish whether the SB firing patterns observed in *TSC2* neurons arise due to changes in synaptic activity as previously reported in our control neurons [27], we probed our cultures with pharmacological agents that modulate glutamate or GABA signalling, applied after 50DPP when SBs patterns had fully established. In agreement with that we found previously, in control neurons inhibition of glutamate signalling via an AMPA receptor antagonist (CNQX) or an NMDA receptor antagonist (APV) lead to a complete abolition of the SB. This was also seen in TSC2 patient derived cultures (Fig. 2C and Fig. S2). Probing the *TSC2* cultures with kainic acid (KA), a drug that mimics the effect of glutamate, resulted in a 3-fold increase in the number of SBs also consistent with what has been previously described in control neurons [28] (Fig. 3C, Fig. S2). Probing the culture with drugs that antagonise GABA receptors, bicuculline or DMCM (6,7-dimethoxy-4-ethyl-beta-carboline-3-carboxylate methyl ester), a negative allosteric modulator of GABAA receptors [29] increased the number of SBs (Fig. 2C and Fig. S2). We also examined the effect of GABA and a GABA positive allosteric modulator on this culture. Previously we showed that application of GABA completely suppressed the SBs in control neurons, here we showed that application of GABA or diazepam, also supressed the SBs in *TSC2* neurons (Fig. 2C and fig. S2). Whereas, exposure to diltiazem, resulted in increasing the number of the SBs, as also seen consistent previously seen for control neurons [27] (Fig. 2C and fig. S2). In all of the previous cases, the patterns of the SBs rapidly recovered after washing the drug out. Taken together, these findings indicate that the SB patterns detected in *TSC2* neurons arise via synaptic activity and that Glutamate (AMPA, NMDA) and GABA signalling are all required for their neuronal network activity.

Synaptic gene *of TSC2* patient iPSC-derived neurons indicates an excitatory/inhibitory imbalance

Having demonstrated that the SB firing patterns in *TSC2* neurons arise from intact synaptic activity, we interrogated whether their abnormal network phenotype could be due an imbalance of excitatory/inhibitory synaptic signalling of the cells. We tested this hypothesis by looking at the expression of a panel of inhibitory and excitatory synaptic markers in *TSC2* and control neurons via qPCR. At the end of the MEA recording period ~60DPP, RNA samples were collected from *TSC2* and control neurons and the expression of various synaptic markers was quantified (Fig. 3).

We quantified mRNA levels for the inhibitory synaptic genes *GAD1* and *GAD2*, which encode distinct GAD (glutamic acid decarboxylase) proteins GAD67 and GAD65, respectively [30]. Our analysis showed a statistically significant increase of approximately 5- and 20-fold changes, respectively in *GAD1* and *GAD2* mRNA levels in *TSC2* neurons as compared to the controls (Fig. 3a, 3b), ($p < 0.05$, unpaired t-test). Likewise, expression of the postsynaptic $GABA_A$ receptor subunits *α1* and *α2* (*GABA-α1* and *-α2*) were also elevated by 2- and 6-fold respectively in *TSC2* neurons (Fig. 3c, 3d), ($p < 0.001$, unpaired t-test). The expression levels of *GRIN2A* and *GRIN2B* which encode the NMDA receptor subunits NR2B and NR2A, respectively [31]; the glutamatergic marker *VGLUT1* which constitutes the main presynaptic vesicular glutamate transporter; the postsynaptic density proteins *PSD95* and *Homer1*, and the presynaptic marker *synaptophysin* [32] were determined. In contrast to the elevation in the mRNA levels of the inhibitory synaptic genes, the levels for the glutamatergic marker *GRIN2A, GRIN2B* and *VGLUT1* showed a clear reduction by approximately 2-, 2- and 14-fold, respectively (Fig. 3e-3g), ($p < 0.01$, unpaired t-test). Genes encoding presynaptic and postsynaptic density proteins were not significantly altered (Fig. 3h-3j), an observation that is consistent with previous reports that showed no significant changes in neuronal morphology or synaptic number in these *TSC2* patient neurons [17]. These findings suggest that at the signalling level there may be an imbalance of excitatory/inhibitory signalling in *TSC2* neurons and is consistent with the effects of decreased glutamate and increased GABA signalling on neuronal network behaviour seen previously.

Chronic inhibition of mTORC1 pathway has no effect on the neuronal network behaviour in *TSC2* patient neurons

Loss of *TSC2* increases mTORC1 activity, we therefore interrogated whether longer-term inhibition of mTORC1 by rapamycin may rescue the neuronal network defects phenotype detected in *TSC2* neurons. Control neurons and *TSC2* neurons were treated with 10nM rapamycin from day 45 of differentiation, and neuronal activity of control and *TSC2* mutant cells was examined at day 40 post plating on MEAs. We did not detect significant alterations in the overall neuronal activity or synchronicity in control neurons treated with rapamycin (fig. S1A), whereas, significant reductions in the basal neuronal activity were seen in *TSC2*-derived neuronal cultures (Fig. 4a). Although rapamycin decreased neuronal hyperactivity of *TSC2* neurons to a comparable level seen in the control firing rate, i.e. a decrease from 0.52 ± 0.09 Hz to 0.13 ± 0.02 in the presence of rapamycin, $p < 0.05$, unpaired t-test, it had no significant effect on SB frequency, SB length or interval (Fig. 4b, 4c, 4d). This indicates that incubation with rapamycin did not rescue the

neuronal synchronicity deficit in *TSC2* neurons. Given that chronic inhibition of the mTORC1 pathway did not increase the number of SBs, we tested whether short-term treatment with rapamycin may have an effect. *TSC2* neurons were treated with rapamycin for 24h and then the neuronal network activity was recorded. Treatment with rapamycin had also no effect on the number of SBs while it decreased the basal excitability of *TSC2* neurons (Fig. S1B). We concluded that both long- and short-term rapamycin treatment was not able to rescue of the abnormal network phenotype of *TSC2* neurons.

Suppression of mTORC1 via ULK1 enhances the neuronal synchronicity in *TSC2* patient-derived neuronal networks

A possible insensitivity to rapamycin treatment could be due insufficient drug activity to effectively restore energy and nutrient homeostasis. In many cell types, rapamycin is reported as being a poor inducer of autophagy, likely due to an incomplete allosteric inhibition of mTORC1 [33]. To explore this notion further, we employed activators of AMPK and ULK1 to better target homeostatic regulation of energy sensing and autophagy, which are both downstream processes that are dysregulated in TSC-diseased cells. *TSC2* cultures were probed with AICAR (an AMPK activator) for 24h and the SB patterns were then determined. Unlike rapamycin, AICAR significantly increased the number of SBs and decreased the SB firing rate in *TSC2* neurons (Fig. 5Bb). However, it did not alter the SB length or interval (Fig. 5Bd) and did not decrease the number of firing spikes outside the SBs (Fig. 5Bc).

As an alternative route to rescue the aberrant *TSC2* phenotype we used an activator of ULK1, LYN-1604 to inhibit mTORC1 through direct phosphorylation of Raptor [34, 35]. Following LYN-1604 treatment for 24 hours and we observed a significant increase in the number of SBs (Fig. 5Bb). The SB number in the presence of LYN-1604 was closely comparable to that observed in control neurons. LYN-1604 also reduced both the SB length and interval, and significantly decreased the number of firing spikes outside the SBs (Fig. 5Bc, 5Bd). Taken together these results show that the defective *TSC2* neuronal networks can be reversed by induction of AMPK and ULK1, two kinases that are fundamentally involved in the regulation of autophagy to restore energy and nutrient homeostasis.

As AICAR and LYN-1604 both improved the synchronicity in *TSC2* neurons, we examined whether probing the culture with any of these drugs would alter the neuronal spatial connectivity. We analysed the correlation matrices between all electrodes of the MEAs for *TSC2* neurons before and after treatment with AICAR and LYN-1604. While treatment with AICAR had no detectable effect on connectivity matrices of the *TSC2* neurons plated on MEAs (Fig. 5C), treatment with LYN-1604 improved the correlation between several electrodes. This effect was presented by increasing the red and dark red pixels between several electrodes in the presence of LYN-1604, an indicative of increasing the neuronal connectivity (Fig. 5C). These findings indicate that the aberrant neuronal connectivity seen in *TSC2* neurons can be restored by activation of ULK1 by LYN-1604 administration.

Discussion

In this report we identify and study abnormal neuronal network behaviour arising in ASD patient iPSC-derived neurons harbouring a *TSC2* mutation. We find that TSC2 patient neurons exhibit increased excitability but lower synchronicity and connectivity. We demonstrate for the first time a route to reverse the defects in TSC2 neuronal synchronicity through the activation of AMPK and ULK1, which would mechanistically inhibit mTORC1 through phosphorylation of Raptor. We propose that these treatments restore network behaviour of *TSC2* patient-derived neurons via change in the intracellular processes that determine the excitatory/inhibitory synaptic balance, adjusting for a high level of GABA signalling at the synapse and reduced level of glutamate transporters of TSC2 patient neurons. In modulating synaptic signalling, the excitatory-inhibitory balance would be restored to normalise SB pattern and neuronal spatial connectivity.

In mouse models, loss of *Tsc1* in all neurons of local cortical circuits or the hippocampus led to neuronal hyperexcitability measured by increased spontaneous neuronal activity and induction of a seizure-like phenotype [36, 37]. The latter phenotype was shown to be due to an excitatory/inhibitory imbalance leading to disinhibition of pyramidal neurons [37]. Knockout of *Tsc1* in mouse neurons also showed clinical and electrographic seizures both spontaneously and under physical stimulation [38]. *TSC*1 KO mice presented with shorten spike bursts, spontaneous periods of desynchronization or frequent high-amplitude sharp waves [38]. We have previously examined the effect of losing one copy of *TSC1* or 2 on neuronal morphology and excitability. We showed that *TSC2*-derived neurons have common neuronal defects caused by both autosomal dominant *TSC1* and *TSC2* mutations and that neuronal hyperexcitability of *TSC* patient-derived cells was reversed by rapamycin [17]. A subsequent study used induced expression *NGN2* to generate excitatory neurons from $TSC2^{+/-}$, $TSC2^{-/-}$ and $TSC2^{+/+}$ cells and replicated the observations on *TSC* neurons hyperexcitability [16].

In that study, as NGN-2 directed neuronal differentiation produces only excitatory neurons it was not possible to monitor aberrant network behaviour arising from an excitatory/inhibitory imbalance [39]. Our current data demonstrates that *TSC2* neurons possess aberrant synchrony and connectivity, in addition to neuronal hyperexcitability described previously [16, 17]. Sundberg et al. found that *TSC2* patient neurons exhibited reduced synaptic activity, measured by a decrease in the number of functional glutamatergic synapses in relation to controls with no effect on the glutamate receptor properties [11]. We report here that reduced synchronicity is consistent with increased GABAergic signalling in an iPSC model. The regulation of coordinated network firing by GABAergic interneurons is well documented and increased GABA signalling activity can suppress the coordination between active and non-active periods in the culture, leading to a significant elevation in the number of spikes outside the SBs. This can explain the patterns of network disorganisation that we observe, manifest as a high number of random and uncorrelated spikes. Furthermore a large reduction in the number of SBs detected in the *TSC2* model was associated with an increase in the burst length, consistent with previous reports in both animal and human models [16, 40]. Our pharmacological profiling demonstrated that consistent with that already shown in control human iPSC-derived neurons and in rodent neurons, glutamate and GABA signalling are the primary drivers for the network activity in *TSC2* neurons [27]. Synchronised bursts detected in *TSC2*

neurons were completely abolished by inhibition of NMDA or AMPA receptors. Conversely, inhibition of $GABA_A$ receptors increased the number of SBs and decreased the SB intervals. This indicates that in our *TSC2* model glutamate signalling still drives the neuronal network activity and GABA signalling shapes the pattern of synchronised activity, as seen in control neurons [27]. Importantly, shifts in excitation or inhibition signalling cause an alteration in the excitability of local circuits leading to an impairment of information processing in the brain and is thought to underlie the pathophysiology of several neuropsychiatric disorders including schizophrenia, ASD and epilepsies [41]. Murine *Tsc1* KO hippocampal hyperexcitability was shown to result from an increase in the balance of inhibitory vs excitatory synapses [37].

The proposal that the aberrant network behaviour observed in *TSC2* neurons is due to increased inhibitory vs excitatory synaptic activity is supported by our RNA analysis. Whilst the genes encoding the markers for synapses including *synaptophysin* and *PSD95*, did not differ from those of the control neurons [42, 43], the expression levels of presynaptic GABA synthesis genes and the postsynaptic $GABA_A$ receptor subunit *a2* were significantly elevated in our *TSC2* model. In contrast, expression of the vesicular glutamate transporter, *VGLUT1* was decreased. This suggests an excitatory/inhibitory synaptic imbalance shifting towards the GABAergic neuronal fate. In line with this observation, hiPSC-derived neurons treated with GABA exhibited a significant reduction in the neuronal synchronicity [27]. This pathophysiological mechanism may connect to the genetics of other syndromic ASD, as *GABAA* receptors, *GAD1* and *GAD2* are all targets of FMRP targets, the genetic cause of Fragile X syndrome [44].

Notably, the neuronal network deficits of *TSC2* neurons was not reversed by rapamycin treatment, a direct inhibitor of mTORC1. Previous studies showed that the effectiveness of rapamycin in control tumour growth for *TSC2* patients, its efficacy in managing neuropsychiatric-associated behaviour in *TSC2* patients has remained unclear [45]. In a report, rapamycin also failed to reverse the enhanced proliferation and altered neurite outgrowth; phenotypes inherent to *TSC* KO NPCs [46]. As rapamycin had little effect on the network deficit, we targeted the aberrant synchronicity and connectivity deficits with alternative approaches, examining upstream *TSC* activation or downstream manipulation the mTORC1 at the molecular level. We found that AMPK activation, and increased phosphorylation of the remaining copy of *TSC2,* increased the number of SBs but the number of spontaneous unsynchronised spiking outside of the SBs remained unaltered and the cultures remained disorganised and less connected. In contrast, the ULK1 activator, LYN-1604b, which inhibits mTORC1 signalling via phosphorylation of Raptor [19], not only increased the number of SBs to a level comparable to that seen in control neurons, but also significantly decreased in the number of spikes outside the SBs and increased in network connectivity. It was therefore the most effective treatment to suppress all aspects of dysfunction network. High mTORC1 activity prevents ULK1 activation by phosphorylating ULK1 at Ser-757 and disrupts its interaction with AMPK, the TSC upstream activator [19]. Treatment with LYN1604 should restore the homeostatic balance of *TSC2* cells. Interestingly, the effective dose for rapamycin to inhibit ULK1 activity via mTORC1 is ~50 nM, five-fold higher than that required to suppress neuronal hyperexcitability of TSC2 patient neurons. At this dose (10 nM) rapamycin had no effect on control neurons [47]. Given that rapamycin is known to

only partially inhibit all the mTORC1-mediated phosphorylation events in cells [33], we propose that ULK1 activation may be a more promising approach to treat the neuronal network deficits of TSC2 patients.

Limitations

A limitation in our study is the number of *TSC2* different patients examined. Although we have identified both a robust and consistent phenotype across multiple independent iPSC clones cultured on different plates and our results point to an improved therapeutic strategy via ULK-1, we currently cannot judge the universality of these observations. In establishing these basic principles, the remaining questions include: how much variation in the specific pattern of network behaviour exists across the TSC2 patient population; is there a difference in both severity and pharmacological response from one patient to the next either arsing due to different *TSC2* mutations or different of polygenic background within their genomes; would the relative effectiveness of ULK-1 and AMPK activation, or even rapamycin inhibition of mTOR vary between patients. To further this study, it will be necessary to greatly expand the size of TSC2, and TSC1, patient cohort for a much larger MEA-based study and include detailed assessment of variation in clinical phenotype.

Conclusions

Taken together, we have used pharmacological approaches to rescue the aberrant neuronal network phonotype linked to TSC2 hypofunction. We have shown that disruption of mTORC1 signalling via ULK1 activation as well as phosphorylation of the remaining copy of TSC2 via AMPK are able to ameliorate synaptic dysfunction in *TSC2* patient-derived neurons. This approach can be used for future development of personalised therapies for these patients.

Abbreviations

AICAR: 5-Aminoimidazole-4-carboxamide ribonucleotide

AMPK: AMP-dependent protein Kinase 1

APV: (2R)-amino-5-phosphonovaleric acid

ASD: Autism Spectrum Disorder

ASDR: Array-Wide Detection Rate

CNQX: 6-cyano-7-nitroquinoxaline-2,3-dione

DMCM: 6,7-dimethoxy-4-ethyl-beta-carboline-3-carboxylate methyl ester

DPP: Days Post Plating

FMRP: Fragile X mental retardation protein

4E-BP1: eukaryotic initiating factor 4E-binding protein 1

GABA: γ-aminobutyric acid

GAD: glutamic acid decarboxylase

GAP: GTPase activating protein

iPSC: induced Pluripotent Stem Cell

KA: Kainic acid

KO: Knockout mouse

rpS6: ribosomal protein S6

S6K1: rpS6 kinase 1

SB: synchronised burst

TSC: Tuberous sclerosis complex

ULK1: Unc-51 like Autophagy Activating Kinase 1

Declarations

Ethics approval and consent to participate

All experiments were exempt from approval of Medical Ethical Toetsingscommissie (METC), Institutional Review Board of the VU medical centre.

Consent for publication

Not applicable

Competing interests

The authors declare that they have no competing interests.

Funding

This work was supported and funded through DEFINE, a Wellcome Trust Strategic Award (100202). VMH is supported by ZonMw (VIDI 917-12-343). The initial concept of this study paper arose from a workshop organised by the European COST Action CA16210 Maximising Impact of research in NeuroDevelopmental DisorderS [MINDDS].

Authors' contributions

MA, VMH and AJH jointly contributed to the conception, design and preparation of the manuscript MA conducted all experimental work and analysis VMH provided the patient and control cells. The authors read and approved the final manuscript.

Acknowledgments

Control and patient lines were generated and characterised by Aishwarya G.Nadadhur and previously published in reference. We thank Prof. Krishna Singh for providing MATLAB imagesc scripts to generate the spatial correlation heat map for the neurons on MEAs. We thank Prof. Andrew Tee for his constructive and helpful comments on a draft of the manuscript.

References

1. Leung AK,Robson WL.Tuberous sclerosis complex: a review. J Pediatr Health Care. 2007; 212: p. 108-14.
2. Huang J,Manning BD.The TSC1-TSC2 complex: a molecular switchboard controlling cell growth. The Biochemical journal. 2008; 4122: p. 179-190.
3. Huang J, Wu S, Wu C-L,Manning BD.Signaling events downstream of mammalian target of rapamycin complex 2 are attenuated in cells and tumors deficient for the tuberous sclerosis complex tumor suppressors. Cancer research. 2009; 6915: p. 6107-6114.
4. Sarbassov DD, Ali SM,Sabatini DM.Growing roles for the mTOR pathway. Current Opinion in Cell Biology. 2005; 176: p. 596-603.
5. Huang J,Manning Brendan D.The TSC1–TSC2 complex: a molecular switchboard controlling cell growth. Biochemical Journal. 2008; 4122: p. 179-190.
6. El-Hashemite N, Zhang H, Henske EP,Kwiatkowski DJ.Mutation in TSC2 and activation of mammalian target of rapamycin signalling pathway in renal angiomyolipoma. The Lancet. 2003; 3619366: p. 1348-1349.
7. Kwiatkowski DJ, Zhang H, Bandura JL, Heiberger KM, Glogauer M, el-Hashemite N,Onda H.A mouse model of TSC1 reveals sex-dependent lethality from liver hemangiomas, and up-regulation of p70S6 kinase activity in Tsc1 null cells. Human Molecular Genetics. 2002; 115: p. 525-534.
8. Zoncu R, Efeyan A,Sabatini DM.mTOR: from growth signal integration to cancer, diabetes and ageing. Nature reviews. Molecular cell biology. 2011; 121: p. 21-35.
9. Normand Elizabeth A, Crandall Shane R, Thorn Catherine A, Murphy Emily M, Voelcker B, Browning C, Machan Jason T, Moore Christopher I, Connors Barry W,Zervas M.Temporal and Mosaic Tsc1 Deletion in the Developing Thalamus Disrupts Thalamocortical Circuitry, Neural Function, and Behavior. Neuron. 2013; 785: p. 895-909.
10. Meikle L, Pollizzi K, Egnor A, Kramvis I, Lane H, Sahin M,Kwiatkowski DJ.Response of a neuronal model of tuberous sclerosis to mammalian target of rapamycin (mTOR) inhibitors: effects on

mTORC1 and Akt signaling lead to improved survival and function. The Journal of neuroscience : the official journal of the Society for Neuroscience. 2008; 2821: p. 5422-5432.

11. Sundberg M, Tochitsky I, Buchholz DE, Winden K, Kujala V, Kapur K, Cataltepe D, Turner D, Han M-J, Woolf CJ, Hatten ME,Sahin M.Purkinje cells derived from TSC patients display hypoexcitability and synaptic deficits associated with reduced FMRP levels and reversed by rapamycin. Molecular psychiatry. 2018; 2311: p. 2167-2183.
12. Tavazoie SF, Alvarez VA, Ridenour DA, Kwiatkowski DJ,Sabatini BL.Regulation of neuronal morphology and function by the tumor suppressors Tsc1 and Tsc2. Nature Neuroscience. 2005; 812: p. 1727-1734.
13. Zeng L-H, Xu L, Gutmann DH,Wong M.Rapamycin prevents epilepsy in a mouse model of tuberous sclerosis complex. Annals of neurology. 2008; 634: p. 444-453.
14. Reith RM, McKenna J, Wu H, Hashmi SS, Cho S-H, Dash PK,Gambello MJ.Loss of Tsc2 in Purkinje cells is associated with autistic-like behavior in a mouse model of tuberous sclerosis complex. Neurobiology of Disease. 2013; 51: p. 93-103.
15. Carson RP, Van Nielen DL, Winzenburger PA,Ess KC.Neuronal and glia abnormalities in Tsc1-deficient forebrain and partial rescue by rapamycin. Neurobiology of disease. 2012; 451: p. 369-380.
16. Winden KD, Sundberg M, Yang C, Wafa SMA, Dwyer S, Chen P-F, Buttermore ED,Sahin M.Biallelic Mutations in TSC2 Lead to Abnormalities Associated with Cortical Tubers in Human iPSC-Derived Neurons. The Journal of Neuroscience. 2019; 3947: p. 9294-9305.
17. Nadadhur AG, Alsaqati M, Gasparotto L, Cornelissen-Steijger P, van Hugte E, Dooves S, Harwood AJ,Heine VM.Neuron-Glia Interactions Increase Neuronal Phenotypes in Tuberous Sclerosis Complex Patient iPSC-Derived Models. Stem Cell Reports. 2019; 121: p. 42-56.
18. Davies DM, de Vries PJ, Johnson SR, McCartney DL, Cox JA, Serra AL, Watson PC, Howe CJ, Doyle T, Pointon K, Cross JJ, Tattersfield AE, Kingswood JC,Sampson JR.Sirolimus Therapy for Angiomyolipoma in Tuberous Sclerosis and Sporadic Lymphangioleiomyomatosis: A Phase 2 Trial. Clinical Cancer Research. 2011; 1712: p. 4071-4081.
19. Kim J, Kundu M, Viollet B,Guan K-L.AMPK and mTOR regulate autophagy through direct phosphorylation of Ulk1. Nature Cell Biology. 2011; 132: p. 132-141.
20. Dunlop EA, Hunt DK, Acosta-Jaquez HA, Fingar DC,Tee AR.ULK1 inhibits mTORC1 signaling, promotes multisite Raptor phosphorylation and hinders substrate binding. Autophagy. 2011; 77: p. 737-747.
21. Lieberthal W,Levine JS.The Role of the Mammalian Target Of Rapamycin (mTOR) in Renal Disease. Journal of the American Society of Nephrology. 2009; 2012: p. 2493-2502.
22. Zheng X, Boyer L, Jin M, Kim Y, Fan W, Bardy C, Berggren T, Evans RM, Gage FH,Hunter T.Alleviation of neuronal energy deficiency by mTOR inhibition as a treatment for mitochondria-related neurodegeneration. eLife. 2016; 5: p. e13378.
23. Warlich E, Kuehle J, Cantz T, Brugman MH, Maetzig T, Galla M, Filipczyk AA, Halle S, Klump H, Schöler HR, Baum C, Schroeder T,Schambach A.Lentiviral Vector Design and Imaging Approaches to

Visualize the Early Stages of Cellular Reprogramming. Molecular Therapy. 2011; 194: p. 782-789.

24. Nadadhur AG, Emperador Melero J, Meijer M, Schut D, Jacobs G, Li KW, Hjorth JJJ, Meredith RM, Toonen RF, Van Kesteren RE, Smit AB, Verhage M,Heine VM.Multi-level characterization of balanced inhibitory-excitatory cortical neuron network derived from human pluripotent stem cells. PloS one. 2017; 126: p. e0178533-e0178533.
25. Livak KJ,Schmittgen TD.Analysis of Relative Gene Expression Data Using Real-Time Quantitative PCR and the 2−ΔΔCT Method. Methods. 2001; 254: p. 402-408.
26. Quiroga RQ, Nadasdy Z,Ben-Shaul Y.Unsupervised Spike Detection and Sorting with Wavelets and Superparamagnetic Clustering. Neural Computation. 2004; 168: p. 1661-1687.
27. Plumbly W, Brandon N, Deeb TZ, Hall J,Harwood AJ.L-type voltage-gated calcium channel regulation of in vitro human cortical neuronal networks. Scientific Reports. 2019; 91: p. 13810.
28. Odawara A, Katoh H, Matsuda N,Suzuki I.Physiological maturation and drug responses of human induced pluripotent stem cell-derived cortical neuronal networks in long-term culture. Scientific Reports. 2016; 61: p. 26181.
29. Puia G, Santi MR, Vicini S, Pritchett DB, Seeburg PH,Costa E.Differences in the negative allosteric modulation of gamma-aminobutyric acid receptors elicited by 4'-chlorodiazepam and by a beta-carboline-3-carboxylate ester: a study with natural and reconstituted receptors. Proceedings of the National Academy of Sciences of the United States of America. 1989; 8618: p. 7275-7279.
30. Grone BP,Maruska KP.Three Distinct Glutamate Decarboxylase Genes in Vertebrates. Scientific reports. 2016; 6: p. 30507-30507.
31. Endele S, Rosenberger G, Geider K, Popp B, Tamer C, Stefanova I, Milh M, Kortüm F, Fritsch A, Pientka FK, Hellenbroich Y, Kalscheuer VM, Kohlhase J, Moog U, Rappold G, Rauch A, Ropers H-H, von Spiczak S, Tönnies H, Villeneuve N, Villard L, Zabel B, Zenker M, Laube B, Reis A, Wieczorek D, Van Maldergem L,Kutsche K.Mutations in GRIN2A and GRIN2B encoding regulatory subunits of NMDA receptors cause variable neurodevelopmental phenotypes. Nature Genetics. 2010; 4211: p. 1021-1026.
32. Wiedenmann B, Franke WW, Kuhn C, Moll R,Gould VE.Synaptophysin: a marker protein for neuroendocrine cells and neoplasms. Proceedings of the National Academy of Sciences of the United States of America. 1986; 8310: p. 3500-3504.
33. Nyfeler B, Bergman P, Triantafellow E, Wilson CJ, Zhu Y, Radetich B, Finan PM, Klionsky DJ,Murphy LO.Relieving Autophagy and 4EBP1 from Rapamycin Resistance. Molecular and Cellular Biology. 2011; 3114: p. 2867-2876.
34. Inoki K, Ouyang H, Zhu T, Lindvall C, Wang Y, Zhang X, Yang Q, Bennett C, Harada Y, Stankunas K, Wang CY, He X, MacDougald OA, You M, Williams BO,Guan KL.TSC2 integrates Wnt and energy signals via a coordinated phosphorylation by AMPK and GSK3 to regulate cell growth. Cell. 2006; 1265: p. 955-68.
35. Egan DF, Shackelford DB, Mihaylova MM, Gelino S, Kohnz RA, Mair W, Vasquez DS, Joshi A, Gwinn DM, Taylor R, Asara JM, Fitzpatrick J, Dillin A, Viollet B, Kundu M, Hansen M,Shaw

RJ.Phosphorylation of ULK1 (hATG1) by AMP-activated protein kinase connects energy sensing to mitophagy. Science (New York, N.Y.). 2011; 3316016: p. 456-461.

36. Zhao J-P,Yoshii A.Hyperexcitability of the local cortical circuit in mouse models of tuberous sclerosis complex. Molecular Brain. 2019; 121: p. 6.
37. Bateup HS, Johnson CA, Denefrio CL, Saulnier JL, Kornacker K,Sabatini BL.Excitatory/inhibitory synaptic imbalance leads to hippocampal hyperexcitability in mouse models of tuberous sclerosis. Neuron. 2013; 783: p. 510-522.
38. Meikle L, Talos DM, Onda H, Pollizzi K, Rotenberg A, Sahin M, Jensen FE,Kwiatkowski DJ.A Mouse Model of Tuberous Sclerosis: Neuronal Loss of Tsc1 Causes Dysplastic and Ectopic Neurons, Reduced Myelination, Seizure Activity, and Limited Survival. The Journal of Neuroscience. 2007; 2721: p. 5546-5558.
39. DeFelipe J.The Evolution of the Brain, the Human Nature of Cortical Circuits, and Intellectual Creativity. Frontiers in Neuroanatomy. 2011; 529.
40. Wang Y, Greenwood JS, Calcagnotto ME, Kirsch HE, Barbaro NM,Baraban SC.Neocortical hyperexcitability in a human case of tuberous sclerosis complex and mice lacking neuronal expression of TSC1. Ann Neurol. 2007; 612: p. 139-52.
41. Tatti R, Haley MS, Swanson OK, Tselha T,Maffei A.Neurophysiology and Regulation of the Balance Between Excitation and Inhibition in Neocortical Circuits. Biological psychiatry. 2017; 8110: p. 821-831.
42. Masliah E, Terry RD, Alford M,DeTeresa R.Quantitative immunohistochemistry of synaptophysin in human neocortex: an alternative method to estimate density of presynaptic terminals in paraffin sections. Journal of Histochemistry & Cytochemistry. 1990; 386: p. 837-844.
43. Koffie RM, Meyer-Luehmann M, Hashimoto T, Adams KW, Mielke ML, Garcia-Alloza M, Micheva KD, Smith SJ, Kim ML, Lee VM, Hyman BT,Spires-Jones TL.Oligomeric amyloid beta associates with postsynaptic densities and correlates with excitatory synapse loss near senile plaques. Proceedings of the National Academy of Sciences of the United States of America. 2009; 10610: p. 4012-4017.
44. Braat S, D'Hulst C, Heulens I, De Rubeis S, Mientjes E, Nelson DL, Willemsen R, Bagni C, Van Dam D, De Deyn PP,Kooy RF.The GABAA receptor is an FMRP target with therapeutic potential in fragile X syndrome. Cell cycle (Georgetown, Tex.). 2015; 1418: p. 2985-2995.
45. Krueger DA, Sadhwani A, Byars AW, de Vries PJ, Franz DN, Whittemore VH, Filip-Dhima R, Murray D, Kapur K,Sahin M.Everolimus for treatment of tuberous sclerosis complex-associated neuropsychiatric disorders. Annals of clinical and translational neurology. 2017; 412: p. 877-887.
46. Martin P, Wagh V, Reis SA, Erdin S, Beauchamp RL, Shaikh G, Talkowski M, Thiele E, Sheridan SD, Haggarty SJ,Ramesh V.TSC patient-derived isogenic neural progenitor cells reveal altered early neurodevelopmental phenotypes and rapamycin-induced MNK-eIF4E signaling. Molecular autism. 2020; 11: p. 2-2.
47. Fan Q-W, Knight ZA, Goldenberg DD, Yu W, Mostov KE, Stokoe D, Shokat KM,Weiss WA.A dual PI3 kinase/mTOR inhibitor reveals emergent efficacy in glioma. Cancer cell. 2006; 95: p. 341-349.

Figures

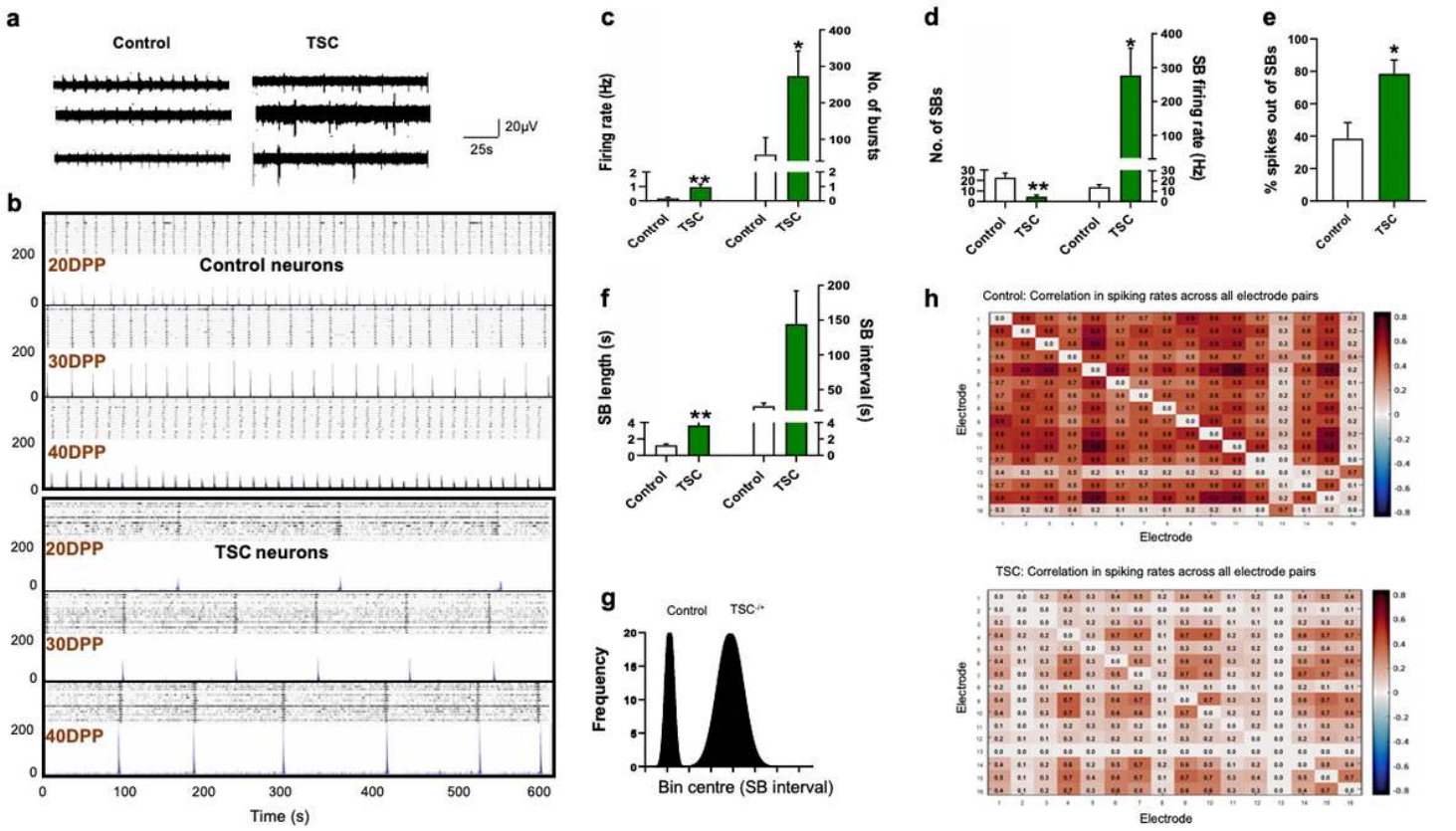

Figure 1

Changes in neuronal activity of TSC2 patient and control neurons recorded with multi electrode arrays (MEAs). (a) Representative voltage traces from three electrodes of the same MEA culture showing the difference in the activity between control and TSC2 neurons at 40DPP (DPP = days post plating). (b) Development of array wide neuronal activity on 20, 30 and 40DPP for control (top) and TSC2 neurons (bottom). For each time point, upper panel shows raster plot and lower panel shows ASDR plot. Vertical scale bars = 200 spikes per 200 ms bin, following 10min of recording. (c) Basal excitability of control and TSC2 neurons showing average spike rate and number of single unit bursts detected. Changes in (d) synchronised burst (SB) activity and the number of spikes in individual SBs, (e) the spikes out of SBs and (f) SB length and interval in control and TSC2 models. (g) Frequency distribution analysis represents the variation in the SB intervals of control neurons TSC2 neurons. (h) Correlation matrices heat map for the control and TSC2 neurons on the MEAs, colours represent the correlation in the firing rates across the indicated electrode. Correlation matrices are calculated for 16 electrodes in control and TCS-/+ neurons plated on the MEAs. Values greater than zero represent positive correlation, while values below zero represent negative correlation. All plots show means ± SEM. *$p < 0.05$, **$p < 0.01$ following unpaired t-tests. Number of cultures = 6 for the control and 8 for TSC2 culture.

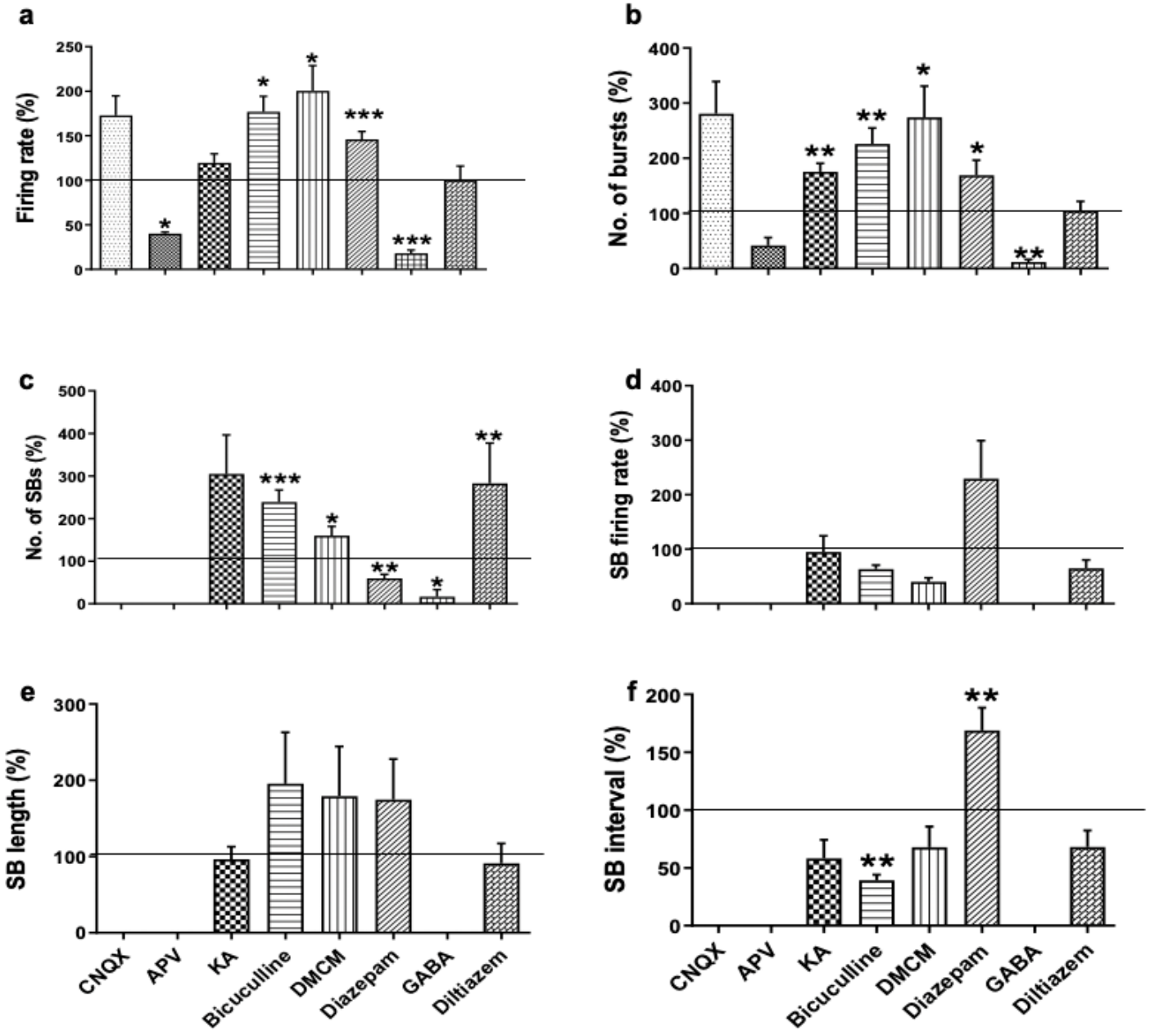

Figure 2

Pharmacological profiling of the network activity of TSC2 neurons. Summary bar plots showing the response of MEA cultures to acute pharmacological treatment: (a, b) basal spike rate and number of single unit bursts following all drug treatments, (c) number of synchronised bursts (SB), (d) SB firing rate and (e) SB length and (f) SB interval following CNQX (50 μM), APV (50 μM), kainic acid (KA) (1 μM), bicuculline (10 μM), DMCM (1 μM), diazepam (50 nM), GABA (1 μM) and diltiazem (5 μM) exposure. All plots show means ± SEM. *p < 0.05, **p < 0.01, ***p < 0.001 following paired t-tests. Number of cultures = 3-10.

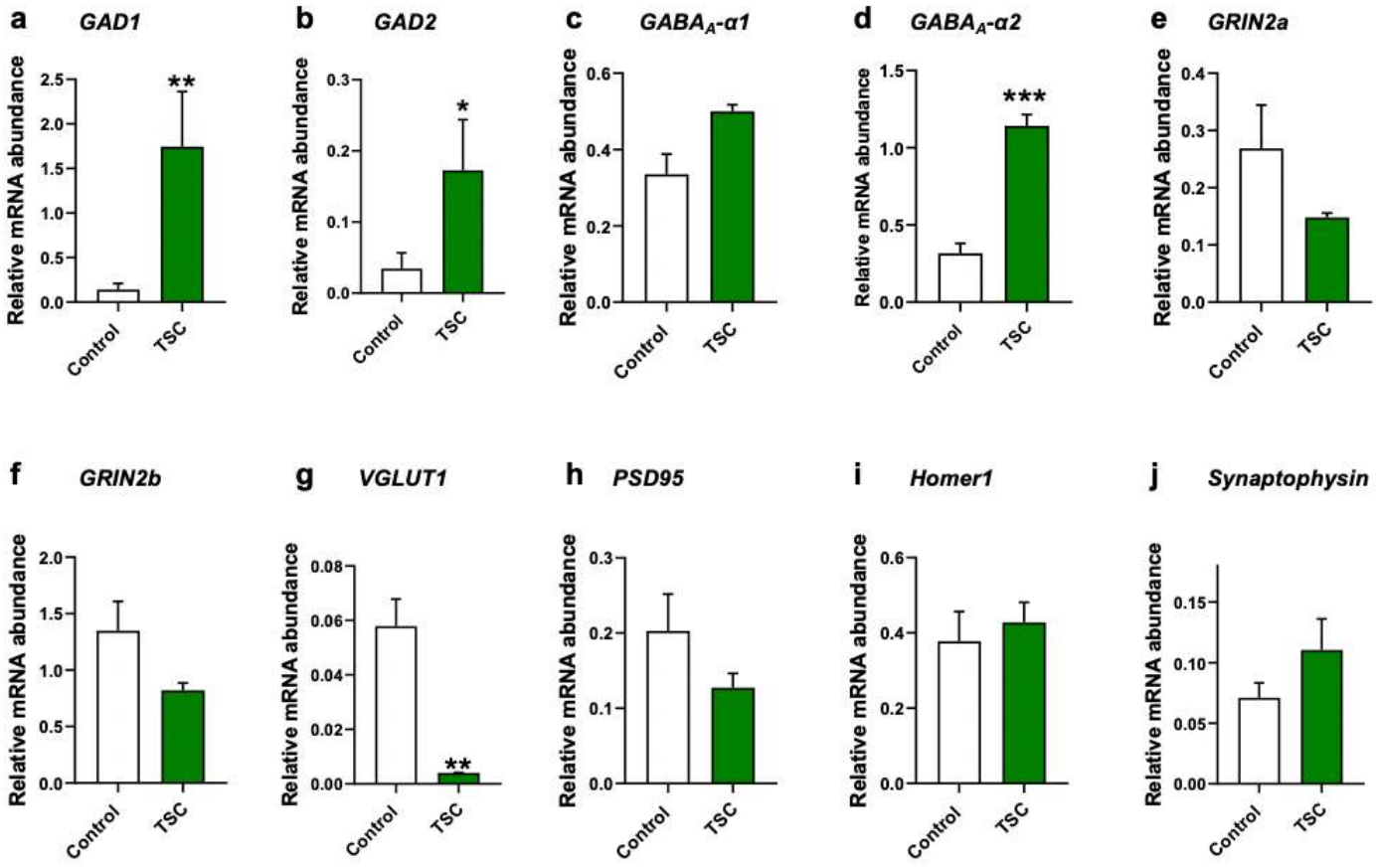

Figure 3

qRT-PCR analysis of synaptic markers in TSC2 neurons at 60DPP. Analysis of a panel of inhibitory and excitatory synaptic markers in control and TSC2 neurons. Data are represented as means ± SEM. *p < 0.05, **p < 0.01, ***p < 0.001 following unpaired t-tests, number of cultures = 6 for control and 3 for TSC neurons.

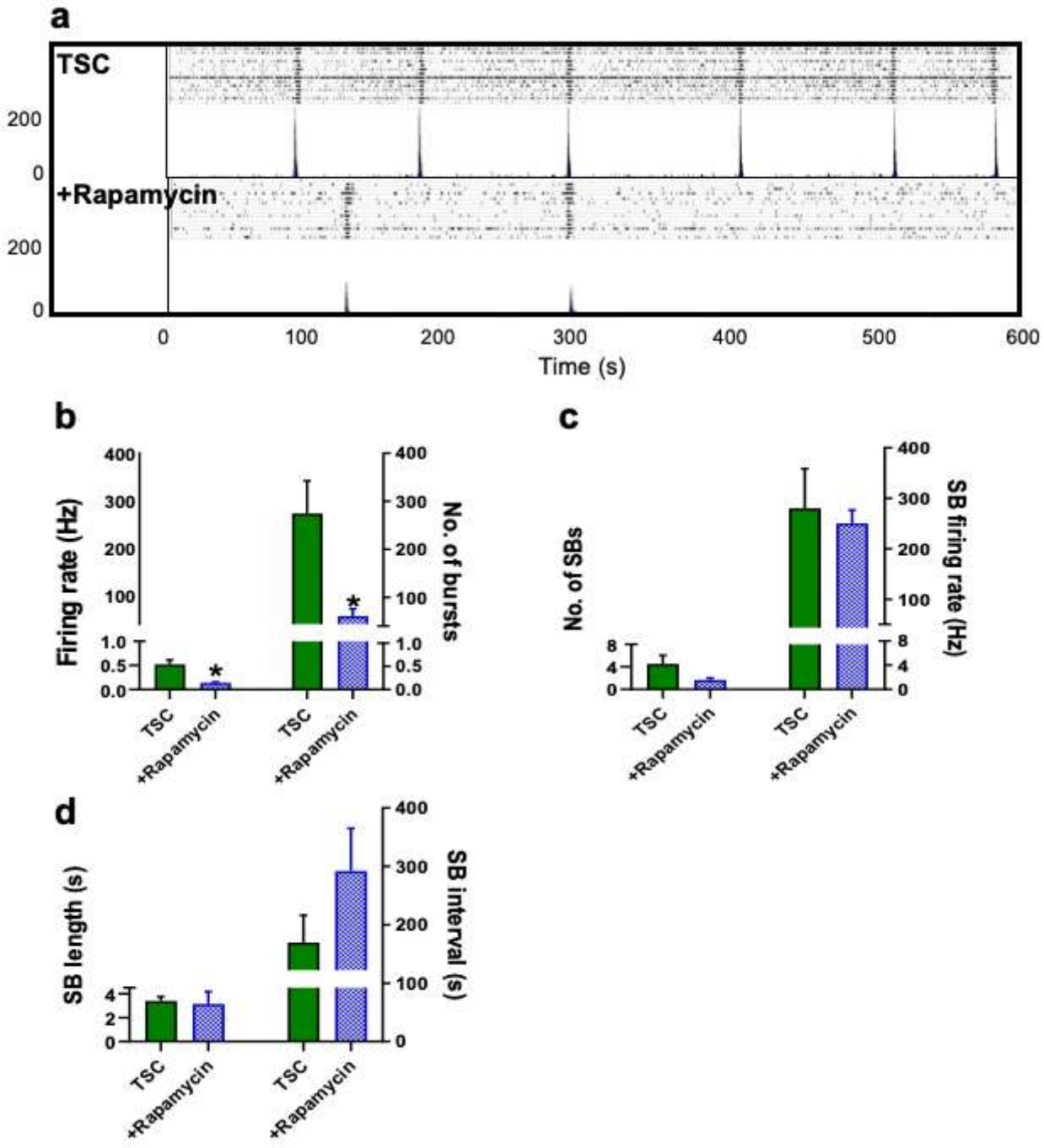

Figure 4

Effects of chronic treatment (55days) with rapamycin on TSC2 neuronal activity. (a) Raster (upper panels) and ASDR plots (lower panels) of a single neuronal MEA culture in the absence and presence of rapamycin (10nM). Vertical scale bar = 200 spikes per 200 ms bin. Changes in (b) basal excitability, (c) synchronised burst (SB) activity and the number of spikes in individual SB, and (d) SB length and interval in the absence and presence of rapamycin. All plots show means ± SEM. *p < 0.05 following unpaired t-tests. Number of cultures = 6.

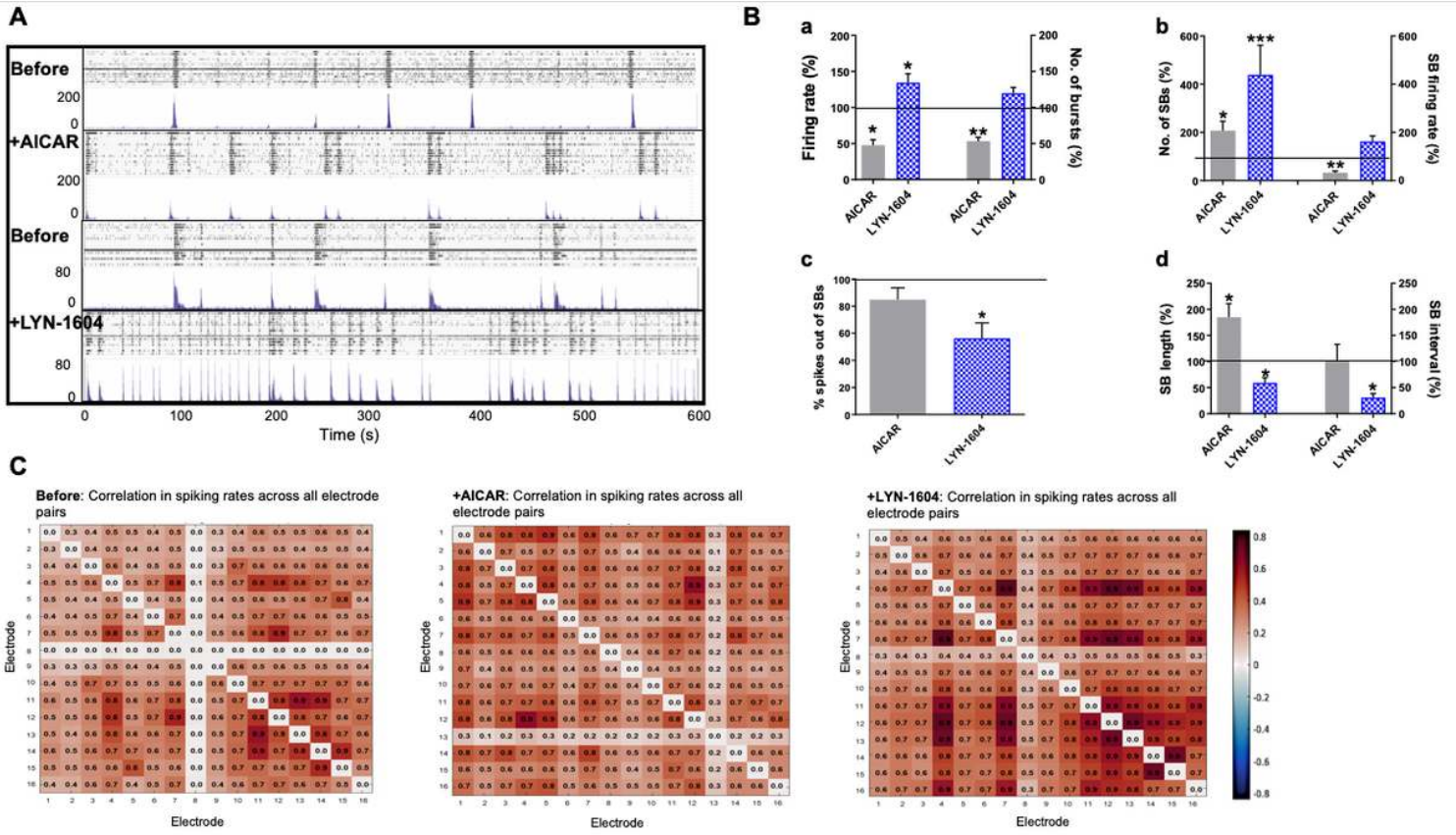

Figure 5

Effects of short-term treatment with upstream or downstream TSC modulators on TSC2 neuronal activity. (A) Raster (upper panel) and ASDR (lower panel) plots of recordings of the same MEA showing the culture-wide response to short-term (24h) exposure to AICAR (1 mM) and LYN-1604 (2 μM). (B) Changes in (a) basal excitability, (b) synchronised burst (SB) activity and the number of spikes in individual SBs, (c) the spikes out of SBs and (d) SB length and interval in the absence and presence of AICAR and LYN-1604, and presented as percentage of the response before the drugs treatment. (C) Correlation matrices heat map for TSC2 neurons in the absence and presence of AICAR and LYN-1604, colours represent the correlation in the firing rates across the indicated electrode. Correlation matrices are calculated for 16 electrodes in control and TCS-/+ neurons plated on the MEAs. Values greater than zero represent positive correlation, while values below zero represent negative correlation. All plots show means ± SEM. *$p < 0.05$, **$p < 0.01$, ***$p < 0.001$ following paired t-tests. Number of cultures = 7.

Supplementary Files

This is a list of supplementary files associated with this preprint. Click to download.

- supplement9.pdf